Annals of Biomedical Engineering, Vol. 42, No. 11, November 2014 (© 2014) pp. 2303–2313
DOI: 10.1007/s10439-014-1041-5

Immunological Analyses of Whole Blood *via* "Microfluidic Drifting" Based Flow Cytometric Chip

Ahmad Ahsan Nawaz,[1] Ruth Helmus Nissly,[2] Peng Li,[1] Yuchao Chen,[1] Feng Guo,[1] Sixing Li,[3] Yasir M. Shariff,[4] Arooj Nawaz Qureshi,[1] Lin Wang,[5] and Tony Jun Huang[1]

[1]Department of Engineering Science and Mechanics, The Pennsylvania State University, University Park, PA 16802, USA; [2]Microscopy and Cytometry Facility, The Huck Institutes of the Life Sciences, The Pennsylvania State University, University Park, PA 16802, USA; [3]Cell and Developmental Biology (CDB) Graduate Program, The Huck Institutes of the Life Sciences, The Pennsylvania State University, University Park, PA 16802, USA; [4]Mechanical Engineering Department, Taibah University, Madina, Saudi Arabia; and [5]Ascent Bio-Nano Technologies Inc., State College, PA, USA

(*Received 26 February 2014; accepted 21 May 2014; published online 4 June 2014*)

Associate Editor Tingrui Pan oversaw the review of this article.

Abstract—Cost-effective, high-performance diagnostic instruments are vital to providing the society with accessible, affordable, and high-quality healthcare. Here we present an integrated, "microfluidic drifting" based flow cytometry chip as a potential inexpensive, fast, and reliable diagnostic tool. It is capable of analyzing human blood for cell counting and diagnosis of diseases. Our device achieves a throughput of ~3754 events/s. Calibration with Flow-Check calibration beads indicated good congruency with a commercially available benchtop flow cytometer. Moreover, subjection to a stringent 8-peak rainbow calibration particle test demonstrated its ability to perform high-resolution immunological studies with separation resolution of 4.28 between the two dimmest fluorescent populations. Counting accuracy at different polystyrene bead concentrations showed strong correlation ($r = 0.9991$) with hemocytometer results. Finally, reliable quantification of CD4+ cells in healthy human blood *via* staining with monoclonal antibodies was demonstrated. These results demonstrate the potential of our microfluidic flow cytometry chip as an inexpensive yet high-performance point-of-care device for mobile medicine.

Keywords—Microfluidics, Flow cytometry, Point of care, Diagnostics, CD4+ counting, Human blood analysis, Mobile medicine.

INTRODUCTION

Healthcare programs have changed recently as clinical labs have become decentralized since the inception of point-of-care (POC) diagnostics.[4,36,40,41,44] Monitoring personal health *via* easy-to-operate, low-cost and yet reliable diagnostic tools can play a vital role in improvement of global healthcare programs, especially in resource-limited settings.[26,29] For example, the home blood glucose testing device has helped millions acquire accurate and fast information about the blood insulin needed to maintain healthy daily activities. However, most other hematological and immunological tests must be performed at centralized clinical labs due to expensive, bulky equipment and skilled operators required for their use.[8–10] Furthermore, two often neglected complications of hematological and immunological tests are the conditions of transport and time required to deliver the sample to the laboratory, which can significantly alter the credibility of the results.[11] Even in otherwise straightforward medical circumstances, inaccurate results can be fatal.

In the last two decades, microfluidics has been envisioned as a potential platform towards achieving reliable POC tools for hematological and immunological tests, with many design approaches tested[1,3,20,21] However, many of these POC devices can only detect one parameter, which limits their widespread applications. In this regard, microfluidic flow cytometry could serve as an excellent alternative due to its ability to perform multi-parametric, high-throughput single cell analysis. For immunological and hematological based diagnostics, flow cytometry is an established and reliable tool.[16–19,30] One popular application is CD4+ cell counting from whole blood of human immunodeficiency virus (HIV)-infected patients, which is extremely important for determining

Address correspondence to Tony Jun Huang, Department of Engineering Science and Mechanics, The Pennsylvania State University, University Park, PA 16802, USA. Electronic mail: junhuang@psu.edu

the appropriate prescription of antiretroviral therapy to combat this infectious disease. Screening tumor biopsies, immunophenotyping, and DNA content analysis are additional applications where flow cytometry is used in cancer diagnostics.[14,34,39] Although flow cytometry is a reliable tool for immunological and hematological based diagnostics, its potential and utility is limited to large centralized institutions due to its many specialized requirements. A bulky footprint, high equipment cost, large consumption of samples and reagents, and requirement for highly skilled personnel for operation and maintenance significantly diminish the conventional flow cytometer's utility as a POC device.[8–10,12,15,16,31,35]

In the past decade, researchers have made significant efforts to developing microfluidics-based miniature flow cytometry devices that can overcome the limitations of traditional benchtop flow cytometers.[2,13,32,33,37,38] One major challenge in this field is to develop techniques that can tightly and precisely focus cells with high cell-focusing precision along both lateral and vertical directions.[5–7,11,16,28] Recently, Lo *et al.*[5] utilized a double-layered device with smaller sample channel height than sheath fluid channels to achieve hydrodynamic focusing. Quake *et al.*[6] demonstrated that by alternately exciting two nearby areas by acousto-optic modulators, time-resolved measurement in a microfluidic channel can be obtained. Di Carlo *et al.*[11] showed that inertial effects in a serpentine-like channel could be exploited to achieve 3D focusing. Recently we developed a "microfluidic drifting" technique that achieved precise 3D hydrodynamic focusing (i.e., submicrometer precision along both lateral and vertical directions) in a simple, single-layered microfluidic device[22,24,27] and a coefficient of variation (CV) of 2.37% with Flow-Check calibration beads. To the best of our knowledge, this is the best CV value that has been achieved by any microfluidic flow cytometer.

In this article, we optimized the performance of our "microfluidic drifting" flow cytometry chip (e.g., use a one-sheath-fluid-inlet device to replace a three-sheath-fluid-inlet device to improve portability) and extended its application from detection of fluorescent beads to immunological analyses of human whole blood. Our on-chip flow cytometer can measure three parameters [forward scatter (FSC), side scatter (SSC) and fluorescent (FL) emission] simultaneously with an on-chip integrated optical fiber based illumination and detection system. We also subjected our flow cytometer to an 8-peak rainbow bead calibration test. In this approach, same-sized (3.4 μm) fluorescent bead populations of eight different intensity values are passed through a flow cytometer to reveal the sensitivity of the system. The 8-peak rainbow bead calibration test is frequently used as a calibration step in clinics and research labs employing flow cytometry and is also used by service engineers to ensure proper laser alignment, light detection, and electronics function when repairing or installing commercial flow cytometers. Next, we performed immunological analysis on human blood from a healthy donor and compared the results to a commercial flow cytometer (Beckman Coulter FC500) for CD4+ lymphocyte cell count. Our results showed good agreement with the results from a commercial flow cytometer,[24] suggesting that this device may be useful as a POC diagnostic tool.

MATERIALS AND METHODS

Device Design and Modeling

A "microfluidic drifting" flow cytometry device with a curvature angle of 180° and three sheath fluid entry points fed from a single sheath fluid inlet (Fig. 1a) was designed to achieve 3D hydrodynamic focusing of cells/particles. Our "microfluidic drifting" device[22,24,27] involves a curved microchannel. When co-injected sheath (*A* in Fig. 1a) and sample-containing (*B* in Fig. 1a) fluids flowed around the curved channel, the induced Dean flow in the curve sweeps the cells/particles in the sample fluid from the top and bottom of the channel towards the center plane of the channel. This step is termed "microfluidic drifting" and effectively focuses the flowing cells/particles in the vertical direction. In the second step, the cells/particles are pushed into a single line by the horizontal sheath flows (*C* and *D* in Fig. 1a). Thus, this two-step procedure results in 3D focusing of the cells/particles within a single-planar microfluidic channel. The footprint of the device measured 16 mm × 26 mm, roughly the same size as a U.S. quarter (Fig. 1b). A channel height of 128 μm was selected to facilitate fiber (125 μm diameter) insertions *via* fiber sleeves, developed along with the channels. We used CFD-ACE+ software (ESI Group) to conduct computational fluid dynamics (CFD) simulations and optimize the device design. Deionized (DI) water was used as sheath fluid and 5 μM fluorescein (abbreviated as "FITC") in DI water was used as sample fluid for initial testing. A relative convergence criterion of 10^{-6} was used in the simulations. We validated the CFD simulation results with experimental results from confocal microscopy. An Olympus IX81 confocal microscope was used for this purpose while 3D image processing was performed by AutoQuant X3 (MediaCybernetics) software.

Device Fabrication

The device was fabricated *via* standard soft-lithography and mold-replica techniques in two steps.[43] SU8

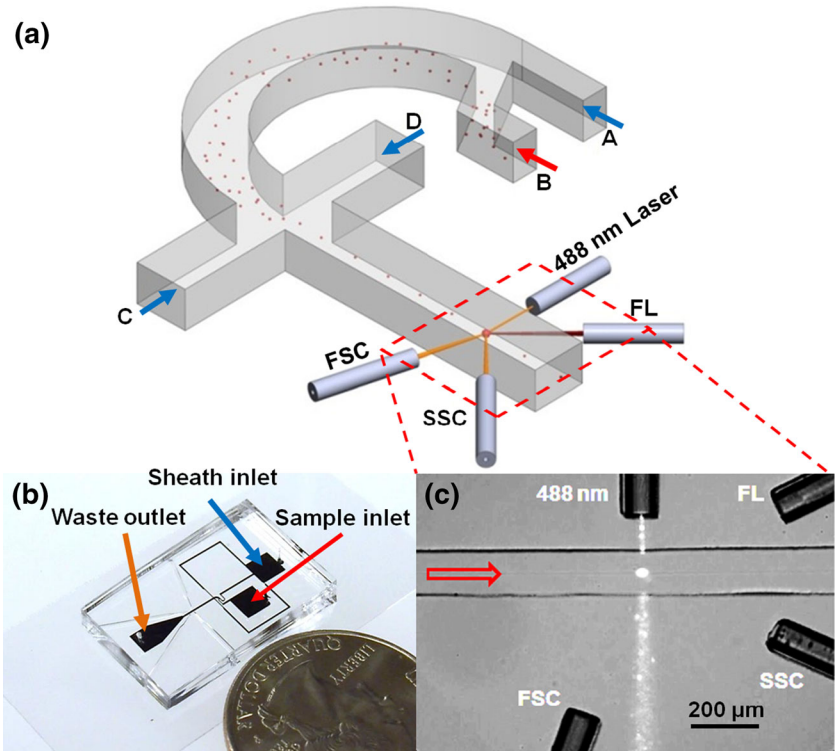

FIGURE 1. "Microfluidic drifting" based flow cytometry device. (a) Schematic of the device indicating the 180º curved region that results in cell/particle focusing and the detection region with input fiber for 488 nm laser and three [forward scatter (FSC), side scatter (SSC), and fluorescence (FL)] detection fibers. A, C, and D are sheath fluid entry points while B represents the sample inlet. The cells/particles focus in the middle vertical plane as they move around the curved channel. The vertically focused cells/particles are then squeezed into a single stream. (b) Small footprint of the device in comparison to a US quarter. The device includes a single inlet for the sheath fluid and a single inlet for sample fluid. (c) Bright-field microscope image of the cells/particles interrogation region [rectangular region in (a)]. Shown is an instant when laser light illuminates a fluorescent 10 μm polystyrene bead as it passes through.

photoresist (~128 μm) was spin-coated on a silicon wafer to develop the master mold. The master mold was salinized with 1H,1H,2H,2H-perfluorooctyl-trichlorosolane vapor (Sigma-Aldrich) so that peel-off of polydimethylsiloxane (PDMS) in the later step is easier. Next, PDMS syrup was poured on the mold followed by degassing to remove all air bubbles. Curing of PDMS was done at 65 °C in an oven to fabricate the microfluidic channel. The PDMS layer was peeled from the mold. A Harris Uni-Core (0.75 mm) was used to punch out the inlets and outlet. Finally, polyethylene tubes were inserted into the inlets and outlet. The inlets were connected to syringe pumps (neMESYS) to supply sheath fluids [sodium dodecyl sulfate (SDS) solution for beads and phosphate buffered saline (PBS) solution for cells] and sample (bead solution or human blood) to the device.

Optical Detection Setup

The fiber-based on-chip optical detection system consisted of one single-mode input fiber (Thorlabs, core diameter = 2.9 μm, NA = 0.14) to direct the laser (Bluesky Research, 10 mW at 488 nm) onto the particles/cells in the main channel. Three detection fibers (Thorlabs, core diameter = 105 μm, NA = 0.22) were used to transmit the light signal captured from particles/cells to the photomultiplier tubes (PMTs; Hamamatsu C6780-20). Two PMTs were fitted with 425 nm filter blocks and one with a 525 ± 10 nm bandpass filter for fluorescent emission detection. Figure 1a depicts the four fiber sleeves for insertion of the laser fiber and three detection fibers. A Nikon (Eclipse *Ti*) optical microscope was used to capture a 20× magnified image of the interrogation region portraying the input fiber, which directs the laser onto the passing particles/cells, and three detection fibers, as shown in Fig. 1c. A commercial flow cytometer (Beckman Coulter FC500) was used for comparison.

Calibration Standards

10 μm Flow-Check Fluorospheres polystyrene (PS) calibration beads (Beckman Coulter, Inc.) were used for characterization of FCS, SSC, and FL signals. To compare its performance with a hemocytometer,

7.32 μm Dragon Green PS beads (Bangs Laboratories, Inc.) with a vendor-reported concentration of 1.5×10^7 were used. Four concentrations of PS beads:SDS (10:990, 50:950, 100:900, and 200:800) were prepared. Each dilution sample was tested on a hemocytometer and our microfluidic flow cytometer for comparison of PS bead counts. For measurement of fluorescence sensitivity, 8-peak Rainbow Calibration Particles (Spherotech) were used, following the manufacturer's instructions.

Sample Preparation

For hematological analysis, fresh venous blood (Zenbio, Inc.) treated with EDTA-anticoagulant was used. A 4 mL blood sample was divided into four equal volumes. Red blood cells (RBCs) were lysed from each 1 mL of blood sample using 1× RBC Lysis Buffer (eBioscience, Inc.) following the manufacturer's suggested protocol. After RBC lysis, the remaining blood cells (white blood cells, or WBCs) were fixed in 1 mL of 4% paraformaldehyde in PBS (Santa Cruz Biotechnology, Inc.) and incubated at room temperature for 10 min. For CD4 staining, two 1 mL blood samples (one for microfluidic flow cytometer and one for commercial flow cytometer) were centrifuged followed by resuspension of WBCs in 400 μL of PBS each. Next, 5 μL of Alexa Fluor 488 labeled anti-human CD4 (clone RPA-T4, BD Biosciences, Inc.) were added to the two samples and then incubated at room temperature for 15 min before analysis on each flow cytometer (our microfluidic device and FC500). WBCs in the remaining two 1 mL volumes were resuspended in 405 μL of PBS to serve as a background fluorescent intensity control in the flow cytometry measurements.

Data Acquisition and Analysis

Data were collected in the microfluidic flow cytometer at a throughput of up to ~3754 events/s and a sample flow rate of 15 μL/min. For calibration beads, 10 s of data were analyzed; however, for whole blood analysis, 6 s of data were collected to match the commercial flow cytometer that was set to record a total of ~20,000 points. In the commercial flow cytometer, a known volume of beads with a known concentration was added to the known volume of blood sample for back-calculating the CD4+ cells in that particular volume of blood. This procedure was adopted because the exact flow rate is not known in this commercial flow cytometer and variable pressure is the factor that decides the flow rate. However, in the microfluidic flow cytometer, as the exact injection flow rate (15 μL/min) is known, the cell count can be known directly without the need of bead addition. The 525 nm fluorescent emission channel was used to detect fluorescent signals from stained CD4+ cells. For the 8-peak rainbow calibration test, the voltage applied to the fluorescent PMT was such that the FITC intensity value for the brightest peak was kept below 10^5, as recommended by the manufacturer.

The output voltage peaks from PMTs were collected *via* digital oscilloscope (Tektronic model DPO400). To calculate CV for FSC, SSC, and FL, we used homemade MATLAB (MathWorks) code. 10% filtering was used to remove the noise from the collected voltage signals. Similarly, 8-peak rainbow calibration test signals were also analyzed with MATLAB code. A predesigned Microsoft Excel file template (Spherotech) was used to determine the Molecules of Equivalent Soluble Fluorochrome (MESF) and calculate the linearity of the detection system. Sensitivity or separation parameter (S) was calculated for the Peak 1 (autofluorescent beads) and Peak 2 (dimmest beads) fluorescence as defined by Woods and Hoffman.[42] S is given by the relation

$$S = \frac{\mu_2 - \mu_1}{\sqrt{SD_2^2 + SD_1^2}},$$

where μ_1 is the mean of the peak 1 fluorescence from auto-fluorescent beads and μ_2 is the mean of the peak 2 fluorescence, while $SD_2^2 + SD_1^2$ is the sum of square of standard deviations from the two peak populations, respectively.

For blood data analysis, FlowJo (Treestar, Inc.) commercial software was used. In particular, the autogating function was employed to analyze the target cells (lymphocytes). For this purpose the CVS files obtained from the oscilloscope were converted to FSC standard file format for flow cytometry. Each dot in the scatter plots represents one particle passing through the laser-interrogation point.

The CD4+ lymphocyte counting experiment on the microfluidic flow cytometer was repeated 10 times with the same blood sample; the same blood sample was analyzed once on the commercial flow cytometer. The presented data indicate the average lymphocyte cells/μL and the standard deviation from the 10 trials.

RESULTS

Device Design Validation

Figure 2a shows the isocurve obtained of 2.5 μM FITC at optimized sample and sheath flow rates (15 and 550 μL/min, respectively). The isocurve profile of the sample fluids indicates a fluid-focusing width of ~4 μm. Using the spray module of CFD-ACE+ software, the behavior of particles in the curved

microfluidic channel was studied numerically. 10 μm particles, representing the size of lymphocytes, were applied to the model and were found to be tightly focused in the middle of the channel (Fig. 2b). Moreover, as particles reached the downstream channel, their single-file behavior was evident from the simulation results (Fig. 2b). We validated the device design and simulation results (Fig. 2b) by confocal microscopy. Figure 2c shows a 6× isometric view of FITC as sample fluid is focused into a focusing width of ~6 μm. The side view of the rectangular dashed area in Fig. 2c is shown in Fig. 2d.

Calibration and Characterization of Detection Signals

We first characterized the performance of our microfluidic flow cytometry device by subjecting it to a standard calibration procedure used for conventional flow cytometers. This step was performed to analyze and calibrate the results from the three channels (FSC, SSC, and FL) by using Flow-Check Fluorospheres. The FSC, SSC, and FL signals were simultaneously collected *via* three optical fibers. The resultant peaks representing individual beads (Figs. 3a–3c) were analyzed to determine the CV of the light scatter signals obtained. Mathematically, standard deviation divided by the mean value of the peak height signifies the CV, which represents the detection resolution of the flow cytometer system. FL, FSC, and SSC displayed CVs of 3.92, 3.82, and 9.81%, respectively, as shown in Figs. 3d–3f. In comparison, CVs from data obtained using the same beads in the commercial flow cytometer (Beckman Coulter FC500) were FL = 1.91%, FSC = 2.14%, and SSC = 6.78%.

Microfluidic Flow Cytometry Calibration

The counting precision of our flow cytometer was compared with a hemocytometer. The graph in Fig. 4 illustrates the count comparison recorded by the hemocytometer and our microfluidic flow cytometer at four concentrations of 7.32 μm PS beads:SDS (10:990, 50:950, 100:900, and 200:800). The count values from the two instruments indicate a correlation value of $r = 0.9991$.

8-Peak Rainbow Calibration

The ability to resolve different fluorescent intensities determines the resolution with which immunological

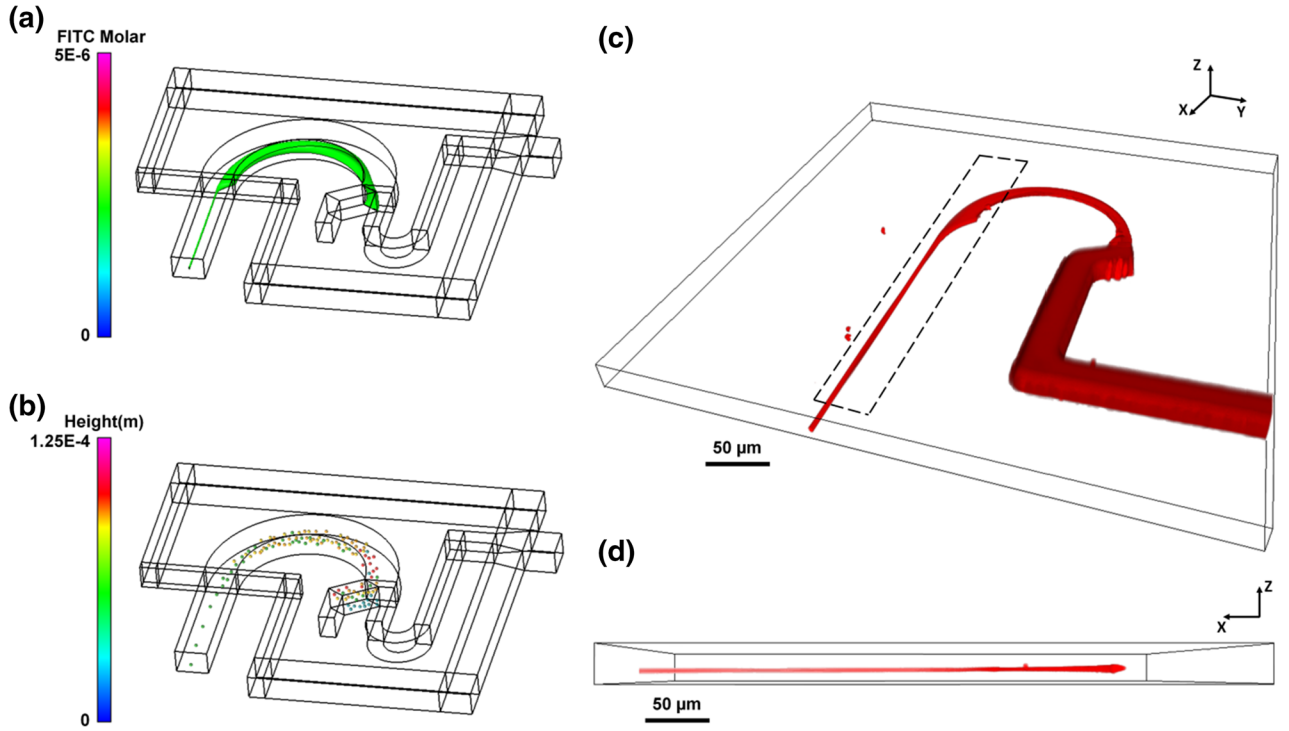

FIGURE 2. Simulation results of the single-sheath-fluid-inlet, "microfluidic drifting" device. (a) Simulation of 5 μM fluorescein (FITC) solution injected into the sheath fluid stream in the device. The isocurve profile (green) indicates that effective three-dimensional (3D) focusing of the sample fluid is achieved. (b) Simulation of 10 μm polystyrene beads focusing into a single-file line of particles as they approach the channel downstream. All downstream particles are green-colored indicating their positioning with respect to height inside the channel. (c) Confocal microscopy Z-stack image using FITC (red) as the sample fluid, indicating excellent 3D focusing. (d) Confocal side-view image of the rectangular dashed region marked in (c). The 3D focusing of the sample fluid in the downstream channel is visible.

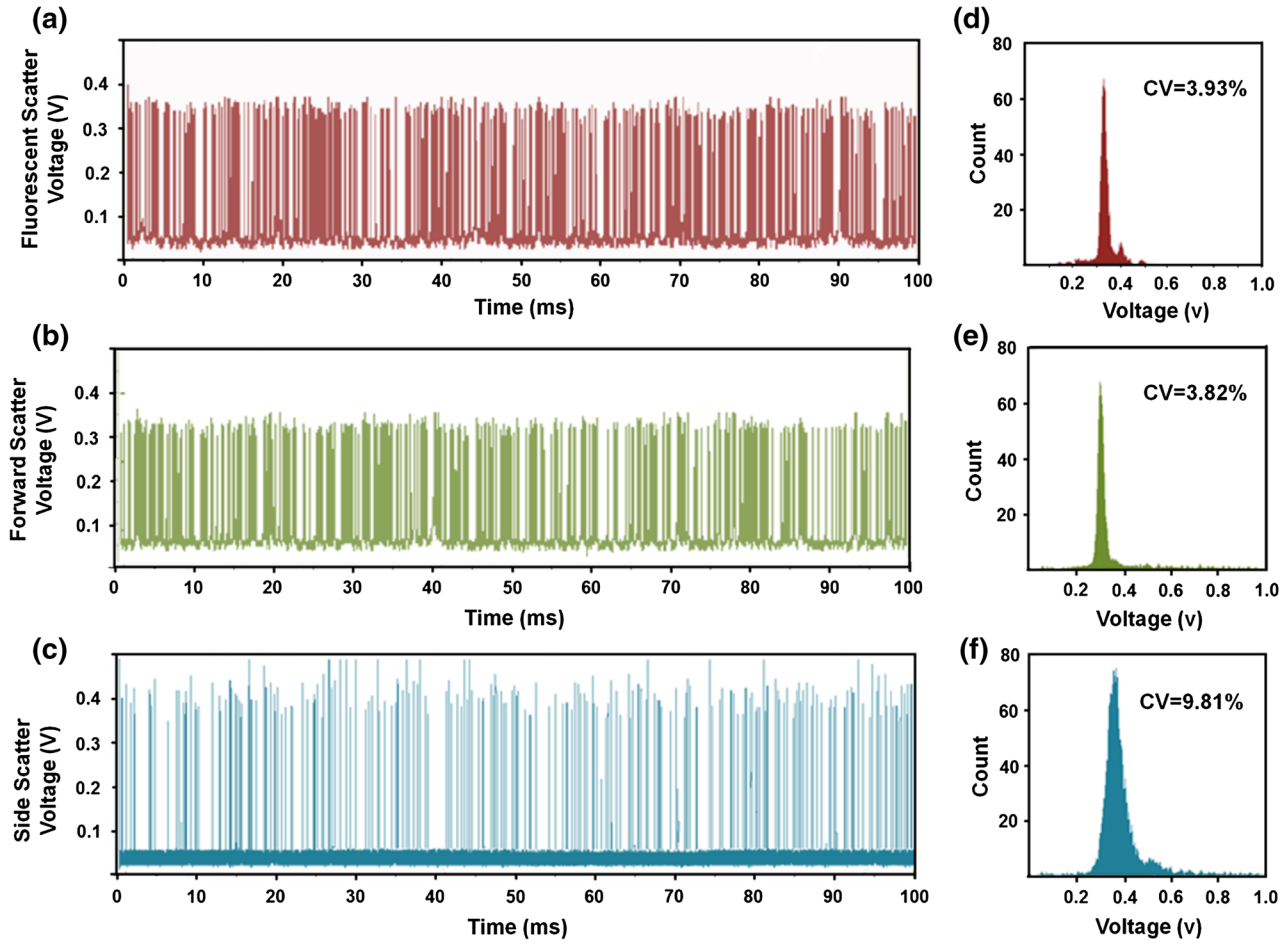

FIGURE 3. Light signals from 10 μm Flow-Check polystyrene calibration beads. (a) FL, (b) FSC, and (c) SSC were collected in photomultiplier tubes. Each peak represents an individual bead that passes through the laser-interrogation region. The peaks collected over a representative timeframe of 100 ms are shown (a–c). The histograms of particle count vs. voltage with respective CVs for FL, FSC, and SSC are depicted in (d–f).

studies can be conducted *via* a particular flow cytometer and is a pivotal strength of flow cytometric based diagnostic analysis. For evaluating this parameter, we used stringent 8-peak rainbow calibration (Spherotech Rainbow Calibration Beads) testing for our microfluidic flow cytometer. Figure 5a represents the histogram of the eight distinct populations of fluorescence intensities. The eight peaks are well separated, and the distribution broadens out as the fluorescence intensity decreases, as expected. To determine the linearity of our microfluidic flow cytometer, we calculated a calibration graph for the FITC (525 nm fluorescence) channel values vs. MESF assigned values by Spherotech. Our flow cytometry chip indicates a correlation value of $r^2 = 0.9833$ which is within the acceptable range according to Spherotech. A separation resolution (S) of 4.28 was calculated for the peak 1 and peak 2 of the rainbow calibration results.

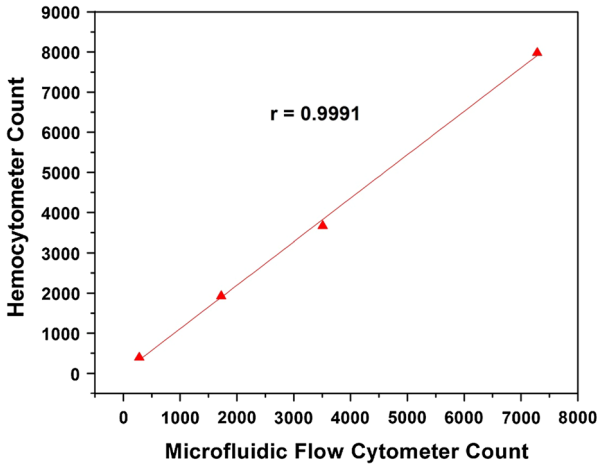

FIGURE 4. PS bead counts at different dilutions using the microfluidic flow cytometer compared with a hemocytometer. Correlation of $r = 0.9991$ indicates good congruency between the count values from hemocytometer and microfluidic flow cytometer.

Human Whole Blood Differentiation

The effectiveness for differentiating subpopulations of human blood by our flow cytometry system was tested next, and results were compared to a commercial flow cytometer. Based on physical properties such as size, refractive index, and granularity, different subpopulations of whole blood appear in different regions hence revealing information useful for diagnosis of diseases. The autogating function of FlowJo software was implemented to objectively identify different subpopulations of blood from the results from the two instruments. Figures 6a and 6b show a comparison of FSC vs. SSC scatter plots of lysed human whole blood recorded from the microfluidic flow cytometer and a commercial flow cytometer. Analyzed results from our microfluidic flow cytometer and a Beckman Coulter FC500 indicated granulocytes (61.8 and 62.4%), monocytes (4.6 and 4.9%), and lymphocytes (25.7 and 26.4%), respectively.

In hematology, information on cell count (i.e., number of cells in a volume of blood) is important and often taken by doctors as a key parameter for deciding on starting a medical procedure/treatment for patients. In particular, CD4+ count in human blood is recognized as an indicator of the strength of the human immune system against HIV. This information is often used to decide a timeline for the start of antiretroviral treatment in HIV-infected patients. In an effort to showcase the ability of our microfluidic flow cytometer to produce reliable cell count results, lysed whole blood stained with monoclonal Alexa Fluor 488-labeled anti-human CD4 antibody was used to perform a CD4+ cell count. CD4+ cells stained with the anti-CD4 antibody were expected to bind to the antibody and therefore emit higher-intensity fluorescence at 525 nm compared with unstained cells or cells lacking CD4 due to the presence of Alexa Fluor 488. FlowJo software was used for gating of lymphocytes to eliminate monocytes, which also express CD4, from the fluorescent signal analysis. As expected, when analyzed on the microfluidic flow cytometer CD4+ lymphocytes displayed increased fluorescence intensity compared with other lymphocytes, as shown in Fig. 7a. The experiment was repeated 10 times to give an average concentration of 858 cells/μL $\pm$ 18.89 (18.4% of lymphocytes), compared with 894 cells/μL (19.2% of lymphocytes) counted *via* a Beckman Coulter FC500 (Fig. 7b). The results show good congruency between the microfluidic cytometry system and the bulky, commercial flow cytometer, which has expensive and specialized peripheral optics and electronics to achieve high-precision results.

DISCUSSION

In this study we characterized the precision, accuracy, and sensitivity of the "microfluidic drifting" flow cytometry device using standardized beads and compared the performance of our device with that of a conventional flow cytometer. The results from our microfluidic flow cytometer showed good agreement with those obtained from the commercial flow cytometer. Furthermore, the microfluidic flow cytometer was demonstrated to perform whole blood analysis and CD4+ lymphocyte counts comparably to a conventional flow cytometer.

Fluidics play a vital role in contributing to the resolution and hence the reliability of a flow cytometer. Our microfluidic flow cytometry device was optimized *via* CFD-ACE+ software (ESI Group) simulations to utilize a single inlet for the sheath fluid to reduce the number of pumps required for sheath fluid injection. This simple approach improves the portability and cost-effectiveness of our device. Comparison of the

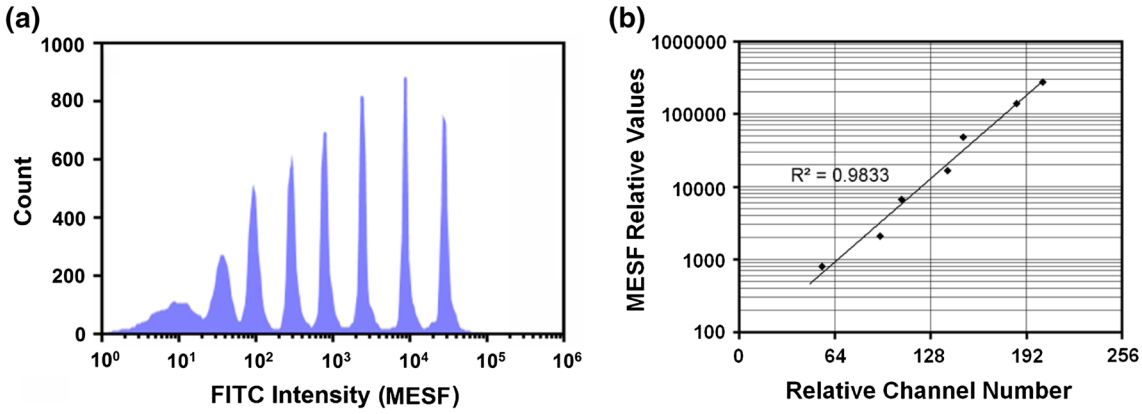

FIGURE 5. (a) Histogram of a suspension of rainbow calibration beads exhibiting eight clear eight populations. The FITC fluorescence intensity is calibrated in MESF scale (Spehrotech). (b) The graph depicts the MESF values assigned by Spherotech Microsoft Excel template compared with the measured FITC values indicating the linearity of our microfluidic flow cytometry device.

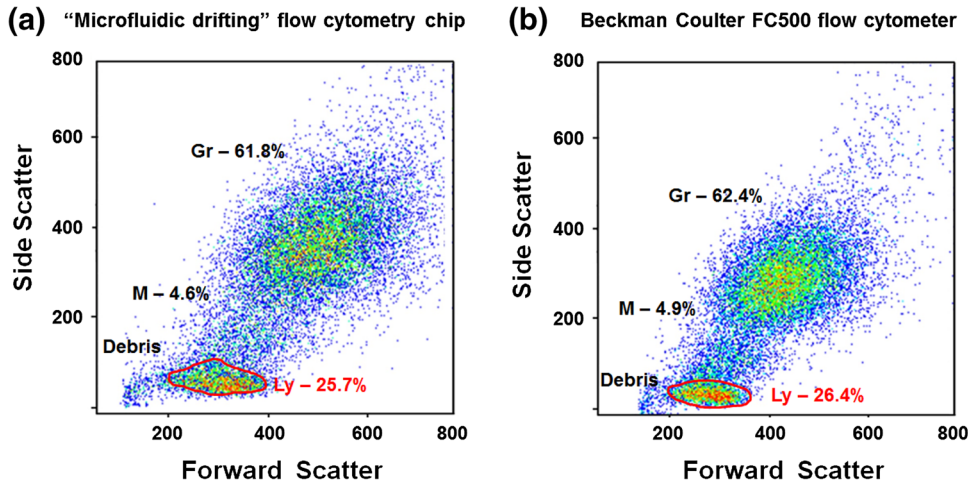

FIGURE 6. Comparison of forward scatter vs. side scatter plot of lysed whole blood from (a) the microfluidic flow cytometer vs. (b) a commercial Beckman Coulter FC500 flow cytometer. Each dot indicates a single cell. Percentages of different subpopulations such as Granulocytes (Gr), Monocytes (M), and Lymphocytes (Ly), red outlined region indicative of general location of these cells, were obtained *via* the autogating function of FlowJo software.

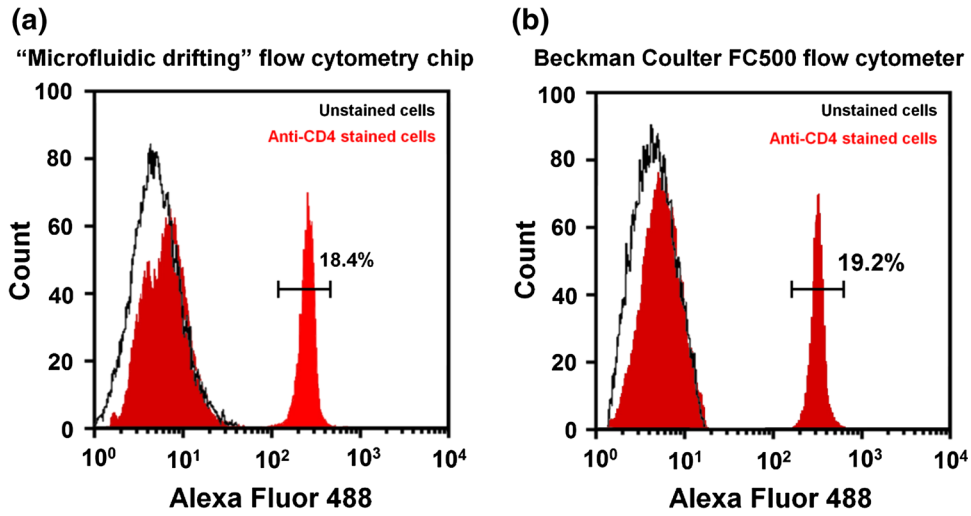

FIGURE 7. Comparison of Alexa Flour 488-labeled anti-CD4 stained whole blood on (a) the microfluidic flow cytometer and (b) a commercial Beckman Coulter FC500 flow cytometer. The black curve represents an unstained control sample of the blood and the colored curves represent the stained sample. Before fluorescence analysis, cells were gated on lymphocytes, as shown in Fig. 6, to exclude monocytes, which also express CD4.

three parameters (FSC, SSC, and FL) of our microfluidic device (FL = 3.93%, FSC = 3.82%, and SSC = 9.81%) to a commercial flow cytometer (FL = 1.91%, FSC = 2.14%, and SSC = 6.78%) show slightly larger CV values. Potential contributors to this increase in CV may be from excess light reflected from channel side walls and possibly undesirable interface of the optical fiber and the PDMS channel.[23,25,45] Moreover, for the analysis of peak data from the oscilloscope, we utilized a MATLAB code, which can perform only basic noise filtering. In the future, we will use integrated data acquisition cards (e.g., USB based or high-speed integrated cards from companies such as CONTEC and Texas Instruments) to eliminate the use of large, expensive oscilloscopes for POC deployment. Furthermore, for a fair comparison we did not use gating for analysis of Beckman Coulter FC500 data. Finer software processing could significantly eliminate the signal noise resulting from doublets, debris, *etc.* (especially due to the gating ability of software such as FlowJo).

The usefulness of flow cytometry in hematology and immunological studies relies on its ability to resolve the fluorescence intensities from immunostaining. The sensitivity of a flow cytometer to resolve dimly fluorescent cells is often measured by subjecting it to an 8-peak rainbow calibration test. In this test, eight populations of similarly sized fluorescent beads stained

with varying amounts of dyes are used to determine a number of factors that affect the sensitivity of the flow cytometry system, including linearity and sensitivity. As a result, from a well-calibrated flow cytometer system of known linearity, the fluorescent staining level of unknown stained cell samples can be calculated. To achieve this, Spherotech has assigned MESF values for each bead's representative peak. After the 8-peak rainbow histogram results were obtained for our device (Fig. 4a), the relative channel number of each of the 8 populations were plotted against the MESF value assigned by Spherotech to obtain the calibration plot as shown in Fig. 4b. Our presented 8-peak rainbow calibration results demonstrate eight distinct populations of fluorescent intensities. The relationship between our device's fluorescence intensity scale and the MESF scale had a correlation value of $r^2 = 0.9833$, indicating an adequate linearity of our flow cytometry system (Fig. 4b).

The eight populations of fluorescent peaks spread progressively from 8 through 1, as expected. However, the first peak (from non-fluorescent beads) and second peak (dimmest) slightly overlapped due to instrumental noise and/or imperfect focusing. Nevertheless, these results indicate that differentiating between cells with weak fluorescence intensity and those with autofluorescence is feasible with our microfluidic flow cytometric device. To quantitatively evaluate the resolution of the peaks 1 and 2, the separation resolution statistic (S) can be used. Our device's S value of 4.28 indicates sensitivity within acceptable range as defined by Woods (>3 is acceptable).[34] These results demonstrate that our microfluidic flow cytometer is able to resolve dim fluorescence even down to 486 MESF value (dimmest peak) while maintaining satisfactory linearity at higher staining levels.

Reliable cell counting is an important aspect of commercial flow cytometers. However, the required addition of counting beads to the target cell sample, as practiced in current flow cytometers, is not only tedious but also expensive. Our microfluidic flow cytometer eliminates this additional step, thus leading to simplicity and ease of operation without affecting the reliability of results. The comparison of PS bead counting with results from a hemocytometer clearly indicates ($r = 0.9991$) the reliability of the counting results from our microfluidic flow cytometer.

Autogating of subpopulations of whole lysed blood data from our microfluidic flow cytometer and the Beckman Coulter FC500 show comparable percentages (Figs. 6a and 6b) of granulocytes, monocytes, and lymphocytes, indicative of our device's potential as a reliable flow cytometer with a much smaller footprint. The comparison of CD4+ lymphocyte cell counting results between our microfluidic flow cytometer and the commercial flow cytometer showed counts from each instrument that were close but indeed exhibited some variations. Since the autogating function of FlowJo software was used for the two flow cytometry data analyses, subjective human gating bias is not responsible. The variations seen in the spread of scatter results and CD4+ lymphocyte enumeration most likely can be explained by the inherent variation of individual flow cytometry instruments, since similar variances in data are also observed between different commercial flow cytometers.[24] Thus, our microfluidic device appears to produce reliable cell counts comparable to a commercial flow cytometer.

In summary, we demonstrate a compact, cost-effective, high-resolution microfluidic-based flow cytometer capable of performing blood analysis with results similar to a large commercial flow cytometer. It has the potential to evolve as an inexpensive POC device that is portable, inexpensive, and simple to use, and requires minimal sample and reagents.

ACKNOWLEDGMENTS

We thank Joseph Rufo and Adem Ozcelik for helpful discussions. This research was supported by the National Institutes of Health (NIH) Director's New Innovator Award (1DP2OD007209-01), National Science Foundation, and the Penn State Center for Nanoscale Science (MRSEC) under grant DMR-0820404. Components of this work were conducted at the Penn State node of the NSF-funded National Nanotechnology Infrastructure Network (NNIN).

REFERENCES

[1]Chen, Y., P. Li, P.-H. Huang, Y. Xie, J. D. Mai, L. Wang, N.-T. Nguyen, and T. J. Huang. Rare cell isolation and analysis in microfluidics. *Lab Chip* 14:626–645, 2014.

[2]Chen, Y., A. A. Nawaz, Y. Zhao, P.-H. Huang, J. P. McCoy, S. J. Levine, L. Wang, and T. J. Huang. Standing surface acoustic wave (SSAW)-based microfluidic cytometer. *Lab Chip* 14:916–923, 2014.

[3]Cheng, X., Y. Liu, D. Irimia, U. Demirci, L. Yang, L. Zamir, W. R. Rodríguez, M. Toner, and R. Bashir. Cell detection and counting through cell lysate impedance spectroscopy in microfluidic devices. *Lab Chip* 7:746–755, 2007.

[4]Chin, C. D., Y. K. Cheung, T. Laksanasopin, M. M. Modena, S. Y. Chin, A. A. Sridhara, D. Steinmiller, V. Linder, J. Mushingantahe, G. Umviligihozo, E. Karita, L. Mwambarangwe, S. L. Braunstein, J. van de Wijgert, R. Sahabo, J. E. Justman, W. El-Sadr, and S. K. Sia. Mobile device for disease diagnosis and data tracking in resource-limited settings. *Clin. Chem.* 59:629–640, 2013.

[5]Chiu, Y.-J., S. H. Cho, Z. Mei, V. Lien, T.-F. Wu, and Y.-H. Lo. Universally applicable three-dimensional hydrodynamic microfluidic flow focusing. *Lab Chip* 13:1803–1809, 2013.
[6]Eyal, S., and S. R. Quake. Velocity-independent microfluidic flow cytometry. *Electrophoresis* 23:2653–2657, 2002.
[7]Goddard, G. R., C. K. Sanders, J. C. Martin, G. Kaduchak, and S. W. Graves. Analytical performance of an ultrasonic particle focusing flow cytometer. *Anal. Chem.* 79:8740–8746, 2007.
[8]Godin, J., C.-H. Chen, S. H. Cho, W. Qiao, F. Tsai, and Y.-H. Lo. Microfluidics and photonics for Bio-System-on-a-Chip: a review of advancements in technology towards a microfluidic flow cytometry chip. *J. Biophotonics* 1:355–376, 2008.
[9]Godin, J., V. Lien, and Y.-H. Lo. Demonstration of two-dimensional fluidic lens for integration into microfluidic flow cytometers. *Appl. Phys. Lett.* 89:061106, 2006.
[10]Godin, J., and Y.-H. Lo. Two-parameter angular light scatter collection for microfluidic flow cytometry by unique waveguide structures. *Biomed. Opt. Express* 1:1472–1479, 2010.
[11]Gossett, D. R., and D. Di Carlo. Particle focusing mechanisms in curving confined flows. *Anal. Chem.* 81:8459–8465, 2009.
[12]Gottwald, E., B. Lahni, G. Lüdke, T. Preckel, and C. Buhlmann. Intracellular HSP72 detection in HL60 cells using a flow cytometry system based on microfluidic analysis. *Biotechniques* 35:358–362, 364, 366–367, 2003.
[13]Grafton, M., L. M. Reece, P. P. Irazoqui, B. Jung, H. D. Summers, R. Bashir, and J. F. Leary. Design of a multistage microfluidics system for high-speed flow cytometry and closed system cell sorting for cytomics. *Proc. SPIE* 6859:1–10, 2008.
[14]Jayat, C., and M. H. Ratinaud. Cell cycle analysis by flow cytometry: principles and applications. *Biol. Cell* 78:15–25, 1993.
[15]Kiesel, P., M. Beck, and N. Johnson. Monitoring CD4 in whole blood with an opto-fluidic detector based on spatially modulated fluorescence emission. *Cytometry A* 79:317–324, 2011.
[16]Kummrow, A., J. Theisen, M. Frankowski, A. Tuchscherer, H. Yildirim, K. Brattke, M. Schmidt, and J. Neukammer. Microfluidic structures for flow cytometric analysis of hydrodynamically focussed blood cells fabricated by ultraprecision micromachining. *Lab Chip* 9:972–981, 2009.
[17]Laerum, O. D., and R. Bjerknes. Flow Cytometry in Hematology. London: Academic Press, 1992.
[18]Lapsley, M. I., L. Wang, and T. J. Huang. On-chip flow cytometry: where is it now and where is it going? *Biomark. Med.* 7:75–78, 2013.
[19]Lee, G.-B., C.-H. Lin, and G.-L. Chang. Micro flow cytometers with buried SU-8/SOG optical waveguides. *Sensors Actuators A Phys.* 103:165–170, 2003.
[20]Maleki, T., T. Fricke, J. Quesenberry, P. Todd, and J. F. Leary. Point-of-care, portable microfluidic blood analyzer system. *Proc. SPIE* 8251:1–3, 2012.
[21]Mao, X., and T. J. Huang. Microfluidic diagnostics for the developing world. *Lab Chip* 12:1412–1416, 2012.
[22]Mao, X., S.-C. S. Lin, C. Dong, and T. J. Huang. Single-layer planar on-chip flow cytometer using microfluidic drifting based three-dimensional (3D) hydrodynamic focusing. *Lab Chip* 9:1583–1589, 2009.
[23]Mao, X., S.-C. S. Lin, M. I. Lapsley, J. Shi, B. K. Juluri, and T. J. Huang. Tunable Liquid Gradient Refractive Index (L-GRIN) lens with two degrees of freedom. *Lab Chip* 9:2050–2058, 2009.
[24]Mao, X., A. A. Nawaz, S.-C. S. Lin, M. I. Lapsley, Y. Zhao, J. P. McCoy, W. S. El-Deiry, and T. J. Huang. An integrated, multiparametric flow cytometry chip using "microfluidic drifting" based three-dimensional hydrodynamic focusing. *Biomicrofluidics* 6:24113–241139, 2012.
[25]Mao, X., J. R. Waldeisen, B. K. Juluri, and T. J. Huang. Hydrodynamically tunable optofluidic cylindrical microlens. *Lab Chip* 7:1303–1308, 2007.
[26]Morris, K. Mobile phones connecting efforts to tackle infectious disease. *Lancet Infect. Dis.* 9:274, 2009.
[27]Nawaz, A. A., X. Zhang, X. Mao, J. Rufo, S.-C. S. Lin, F. Guo, Y. Zhao, M. Lapsley, P. Li, J. P. McCoy, S. J. Levine, and T. J. Huang. Sub-micrometer-precision, three-dimensional (3D) hydrodynamic focusing via "microfluidic drifting". *Lab Chip* 14:415–423, 2014.
[28]Oakey, J., R. W. Applegate, E. Arellano, D. Di Carlo, S. W. Graves, and M. Toner. Particle focusing in staged inertial microfluidic devices for flow cytometry. *Anal. Chem.* 82:3862–3867, 2010.
[29]Pop-Eleches, C., H. Thirumurthy, J. P. Habyarimana, J. G. Zivin, M. P. Goldstein, D. de Walque, L. MacKeen, J. Haberer, S. Kimaiyo, J. Sidle, D. Ngare, and D. R. Bangsberg. Mobile phone technologies improve adherence to antiretroviral treatment in a resource-limited setting: a randomized controlled trial of text message reminders. *AIDS* 25:825–834, 2011.
[30]Shapiro, H. M. Practical Flow Cytometry. New York: Wiley-Liss, 2003.
[31]Shapiro, H. M., and N. G. Perlmutter. Violet laser diodes as light sources for cytometry. *Cytometry* 44:133–136, 2001.
[32]Shi, J., X. Mao, D. Ahmed, A. Colletti, and T. J. Huang. Focusing microparticles in a microfluidic channel with standing surface acoustic waves (SSAW). *Lab Chip* 8:221–223, 2008.
[33]Shi, J., S. Yazdi, S.-C. S. Lin, X. Ding, I.-K. Chiang, K. Sharp, and T. J. Huang. Three-dimensional continuous particle focusing in a microfluidic channel via standing surface acoustic waves (SSAW). *Lab Chip* 11:2319–2324, 2011.
[34]Skommer, J., J. Akagi, K. Takeda, Y. Fujimura, K. Khoshmanesh, and D. Wlodkowic. Multiparameter Lab-on-a-Chip flow cytometry of the cell cycle. *Biosens. Bioelectron.* 42:586–591, 2013.
[35]Telford, W. G., T. S. Hawley, and R. G. Hawley. Analysis of violet-excited fluorochromes by flow cytometry using a violet laser diode. *Cytometry A* 54:48–55, 2003.
[36]Tudos, A. J., G. J. Besselink, and R. B. Schasfoort. Trends in miniaturized total analysis systems for point-of-care testing in clinical chemistry. *Lab Chip* 1:83–95, 2001.
[37]Wang, J., B. Fei, R. L. Geahlen, and C. Lu. Quantitative analysis of protein translocations by microfluidic total internal reflection fluorescence flow cytometry. *Lab Chip* 10:2673–2679, 2010.
[38]Wang, J., Y. Zhan, N. Bao, and C. Lu. Quantitative measurement of quantum dot uptake at the cell population level using microfluidic evanescent-wave-based flow cytometry. *Lab Chip* 12:1441–1445, 2012.
[39]Wang, J.-H., L. Cheng, C.-H. Wang, W.-S. Ling, S.-W. Wang, and G.-B. Lee. An integrated chip capable of performing sample pretreatment and nucleic acid amplification

for HIV-1 detection. *Biosens. Bioelectron.* 41:484–491, 2013.
[40]Wang, S., F. Inci, G. De Libero, A. Singhal, and U. Demirci. Point-of-care assays for tuberculosis: role of nanotechnology/microfluidics. *Biotechnol. Adv.* 31:438–449, 2013.
[41]Wei, F., R. Lam, S. Cheng, S. Lu, D. Ho, and N. Li. Rapid detection of melamine in whole milk mediated by unmodified gold nanoparticles. *Appl. Phys. Lett.* 96:133702, 2010.
[42]Woods, J., and R. Hoffman. Evaluating fluorescence sensitivity on flow cytometers: an overview. *Cytometry A* 33:256–259, 1998.
[43]Xia, Y., and G. M. Whitesides. Soft Lithography. *Annu. Rev. Mater. Sci.* 28:153–184, 1998.
[44]Yager, P., G. J. Domingo, and J. Gerdes. Point-of-care diagnostics for global health. *Annu. Rev. Biomed. Eng.* 10:107–144, 2008.
[45]Zhao, C., Y. Liu, Y. Zhao, N. Fang, and T. J. Huang. A reconfigurable plasmofluidic lens. *Nat. Commun.* 4:2305, 2013.